Accuracy of the pseudopotential approximation in *ab initio* theoretical spectroscopies

Eleonora Luppi,[1,2] Hans-Christian Weissker,[1,2] Sandro Bottaro,[2,3] Francesco Sottile,[1,2] Valérie Veniard,[1,2] Lucia Reining,[1,2] and Giovanni Onida[2,3]

[1]*Laboratoire des Solides Irradiés, École Polytechnique, CNRS-CEA/DSM, F-91128 Palaiseau, France*

[2]*European Theoretical Spectroscopy Facility (ETSF)*

[3]*Dipartimento di Fisica, Università di Milano, Via Celoria 16, 20133 Milan, Italy*

(Received 5 August 2008; revised manuscript received 4 November 2008; published 31 December 2008)

A large number of today's *ab initio* calculations, in particular in solid-state physics, are based on density-functional theory using first-principles pseudopotentials. This approach, initially developed for the ground state, is nowadays widely used as a starting point for the calculation of excited-state properties, as, for instance, those involved in optical spectroscopy. In this paper we investigate the validity and the accuracy of the pseudopotential approximation, analyzing how different choices within the latter can influence the calculated electronic response of silicon and silicon carbide. We consider norm-conserving first-principles pseudopotentials, both in the fully nonlocal (Kleinman-Bylander) and the semilocal forms, with different choices for the reference (local) component. The effects of the inclusion of outer-core states in the valence shell are analyzed in order to obtain a detailed comparison with all-electron calculations. We present accurate results for different pseudopotential descriptions of Kohn-Sham and quasiparticle band structures and of many spectroscopic quantities in the linear and the nonlinear response regimes for different momentum transfers **Q**. Moreover, the effects of the pseudopotential nonlocality have been analyzed for electron-energy-loss spectra in the limit of vanishing momentum transfer. Our results show that the pseudopotential approximation can be quite safely applied to excited-state calculations, even when they involve Kohn-Sham eigenvalues and eigenvectors several tens of eV above the Fermi energy.

DOI: 10.1103/PhysRevB.78.245124 PACS number(s): 78.20.Bh, 42.70.Nq, 71.10.−w

I. INTRODUCTION

Over the last years, the number of *ab initio* calculations of electronic spectra on more and more complex systems has increased impressively.[1–4] Most of these calculations are based on density-functional theory within the Kohn-Sham scheme (DFT-KS) in the pseudopotential approximation (PA).[5–8]

The success of the PA is due to the fact that it enables the study of very complex large-scale systems, by removing the core electrons from the calculations and treating only the valence electrons, which are the chemically active players. In the PA, the core electrons are frozen and the electron-ion Coulomb interaction for the valence electrons is replaced by an effective (semilocal or fully nonlocal) potential. The valence electrons move hence in a potential which, in the core region, is much softer than the bare Coulomb potential. The pseudopotentials (PPs) are constructed in order to reproduce the true electron wave functions outside the core region defined by a cutoff radius r_c.

Several different procedures for constructing *ab initio* norm-conserving pseudopotentials (NCPPs) have been proposed. The most important ones are the Bachelet-Hamann-Schlüter (BHS),[5] the Hamann,[6] and the Troullier-Martins schemes.[7] Furthermore, starting from the resulting semilocal pseudopotentials, a very commonly employed approach leading to fully nonlocal pseudopotentials and a separable Hamiltonian was introduced by Kleinman and Bylander[8] (KB). The separability makes the KB approach very convenient from the computational point of view, which is the reason for its large success in today's electronic-structure and total-energy calculations.

Over the last decade, pseudopotential DFT-KS has also become a common starting point for *ab initio* excited-state calculations, such as the description of quasiparticle properties of solids within the first-principles *GW* approximation and optical properties within many-body perturbation theory (*GW*-Bethe-Salpeter equation)[9–14] or the time-dependent density-functional theory (TDDFT).[13,15–20] Different works which calculate *GW* quasiparticle energies using the PA can be found in literature, from the seminal work of Hybertsen and Louie[12] up to the work of Bruneval *et al.*,[2] who went beyond *GW* by including vertex corrections in the self-energy. Many calculations of linear and nonlinear spectra are based on the PA, such as the work of Weissker *et al.*,[21] where a combination of TDDFT and a many-body approach is successfully used to compute the dynamical structure factor of silicon, or for nonlinear spectra, the work of Leitsmann *et al.*,[22] who presented a way to include excitonic effects in the calculation of the second-harmonic generation (SHG).

In this kind of calculation which involves electron states of energies ranging well above the Fermi level, the assumptions and approximations within the PA are often uncritically used. However, the PA and the PP construction schemes have been developed in particular for ground-state (GS) calculations. Only later have they been applied to calculations in the optical range. Therefore the underlying assumptions and approximations need to be verified for the more demanding situations mentioned above.

In the present paper, we verify the validity of the PA and study the influence of different choices in the construction of the PP on different spectra. The semilocality and full separability (Kleinman-Bylander form) of a pseudopotential and other commonly used approximations are studied via a detailed analysis of the DFT-KS band structure and subsequent calculations of response functions. The effects on the inverse

dielectric function, appearing in the calculation of the screening in the *GW* scheme and of the electron-energy-loss spectra (EELS), are investigated for different pseudopotential descriptions.

Within the PA, the semilocal and fully nonlocal forms of a PP are assumed to give equivalent physical results. In isolated atoms the two give by definition the same results. However, a detailed verification has never been done before.

An additional problem arises for pseudopotentials in the Kleinman-Bylander form because the KB Hamiltonian does not obey the Wronskian theorem. This can lead to eigenfunctions that are not energetically ordered according to the number of nodes.[23] For this reason, spurious bound states, called *ghost states*,[24,25] can appear. We investigate the effects of such ghost states in an extended energy region.

Furthermore, both the calculation of response functions and the calculation of excited states in the framework of many-body perturbation theory, such as *GW* calculations, include sums over transitions in which matrix elements appear. When calculated in real space, these matrix elements are integrals over the extension of the wave functions including the core region. As the PA implies a poor description of the core region, its validity is linked to the importance of the latter. The core region can in principle affect the calculation of the matrix elements, e.g., in the evaluation of the dielectric properties.[26] Some investigations of the resulting error exist for isolated atoms,[27] where it has been shown to be small. However, the same conclusion cannot be trivially generalized when atoms are put in a different chemical environment.

In fact, the validity of the PA has recently been brought into question.[28–34,36] Kageshima and Shiraishi[37] proposed a correction to the PA for the calculation of momentum matrix elements, improving the description of the core region. Later, different and more sophisticated approaches to bypassing the above problems were proposed. The main schemes are the use of all-electron (AE) valence wave functions, as in the projector augmented wave (PAW) approach,[28–35] and the multiprojector method.[36]

Direct comparisons of the optical properties of semiconductors obtained within the PAW approach and within the PA were presented by Adolph *et al.*,[28] showing that the main differences between the two approaches are related to the localization of core states: the more that the core states are localized, close to the nucleus, the more that the pseudopotential calculations are reliable. Therefore it is reasonable to assume that PP results improve when more electrons are included in the valence region and the remaining core contains only very deep and localized levels.

Pseudopotential issues in self-energy calculations have been discussed by Lebègue *et al.*[33] comparing *GW* gaps obtained within the all-electron PAW method with PA ones and showing that some differences arise. In particular the PAW method is found to decrease the gaps. It is therefore argued that the PA fortuitously improves the agreement with experiment.

In the present paper we analyze in detail the possible sources of errors when the PA is used for the calculations of excited states. To improve toward an all-electron description, which is exempt from the drawbacks mentioned above, we consider a pseudopotential where the outer-core electrons are explicitly considered within the valence.

In order to study the overall effect of the PA on the dielectric response we study spectra related to different spectroscopies, for both zero and nonzero momentum transfers. For vanishing momentum transfer, another problem arises from the pseudopotential nonlocality (both in the KB form and in the non-KB form). The nonlocality complicates the evaluation of dipole matrix elements. While for finite momentum transfer $\mathbf{q}$ the matrix elements of the operator $e^{-i\mathbf{qr}}$ are always well defined, in the long-wavelength limit $e^{-i\mathbf{qr}} = 1 - i\mathbf{qr}$, one is lead to consider matrix elements of the position operator $\mathbf{r}$, which in periodic systems is ill defined. The matrix elements of the position operator must therefore be calculated via the velocity operator (i.e., the commutator between the Hamiltonian and the position operator) which is not proportional to the momentum $\mathbf{p}$, but includes also an additional term proportional to the commutator $[V_{\mathrm{nl}}, \mathbf{r}]$,[38,39] where V_{nl} is the nonlocal part of the pseudopotential.

Finally, the effects of the PA have also been studied beyond the linear response. In fact, the theoretical description of nonlinear processes in solids is a formidable task, and important difficulties have delayed any accurate calculations for many years.[22,40] In this difficult framework, the influence of pseudopotentials on the nonlinear spectra has to be analyzed carefully. All calculations have been performed for Si and cubic SiC semiconductor crystals, which are well characterized experimentally and for which several theoretical results exist in the literature.

The paper is organized as follows. In Sec. II, after a brief summary of the main issues involved in first-principles pseudopotential theory, approximations, and possible problems, we review the technical details of semilocal and fully nonlocal (separable) pseudopotentials, including the choice of the "reference" angular component, and we define the set of pseudopotentials considered in this work. In Sec. III we present our results for the logarithmic derivatives (LDs) and for the Kohn-Sham eigenvalues and eigenfunctions, addressing specifically the local-density approximation (LDA) band structure. In Sec. IV we address quasiparticle energies computed within the *GW* approximation of Hedin.[41] Subsequently, in Sec. V we study absorption spectra and the loss function. Results for zero and nonzero momentum transfers $\mathbf{Q}$ are presented, comparing the use of different pseudopotential schemes and analyzing the influence of the $[V_{\mathrm{nl}}, \mathbf{r}]$ commutator on the resulting spectra. Finally, results beyond the linear response, namely, for second-harmonic generation, are presented in Sec. VI.

II. PSEUDOPOTENTIAL DETAILS

A. Theory

We start from the usual expression for a NCPP written, in principle, as an infinite sum of nonlocal terms,

$$V^{\mathrm{PP}}(\mathbf{r},\mathbf{r}') = \sum_{l=0}^{+\infty} v_l(r,r')\hat{P}_l(\Omega,\Omega'). \tag{1}$$

Here $\hat{P}_l$ is the angular momentum projection operator. Usually, one assumes that all terms corresponding to angular

TABLE I. Atomic parameters used for generating the standard and the outer-core PPs. The cutoff radii are given in bohr.

		r_{cut} (a.u.)				r_{cut} (a.u.)		
	Ref. configuration Neutral	s	p	d	Ref. configuration Excited-ionized	s	p	d
Standard	$3s^2 3p^2 3d^0$	1.05	1.27	1.27	$3s^1 3p^{0.75} 3d^{0.25}$	1.00	1.10	0.95
Outer-core	$2s^2 2p^6 3s^2 3p^2 3d^0$	0.58	0.70	1.27	$2s^2 2p^6 3s^1 3p^{0.75} 3d^{0.25}$	0.58	0.70	1.20

momenta larger than a chosen value $l_{\max}$ can be well approximated by one and the same v_l, called the *reference component* $v_{l\mathrm{ref}}$ of the pseudopotential. In this way, the pseudopotential can be set up in terms of an angular momentum–dependent part plus a local term. Considering Eq. (1) and the assumptions described above,

$$\begin{aligned} V^{\mathrm{PP}} &= \sum_{l=0}^{l=l_{\max}} v_l \hat{P}_l + \sum_{l=l_{\max}+1}^{+\infty} v_l \hat{P}_l \\ &= \sum_{l=0}^{l=l_{\max}} [v_l - v_{l\mathrm{ref}}]\hat{P}_l + \sum_{l=l_{\max}+1}^{+\infty} v_l \hat{P}_l + v_{l\mathrm{ref}} \sum_{l=0}^{l=l_{\max}} \hat{P}_l \\ &\approx \sum_{l=0}^{l=l_{\max}} [v_l - v_{l\mathrm{ref}}]\hat{P}_l + v_{l\mathrm{ref}} = v_{\mathrm{nloc}} + v_{l\mathrm{ref}}, \end{aligned} \tag{2}$$

where the dependence on $\mathbf{r}$ and $\mathbf{r}'$ is the same as in Eq. (1). In this way, the use of angular momentum projectors is limited to a few small-l components.

The explicit expression of the nonlocal term in real-space representation is

$$v_{\mathrm{nloc}}(r,r',\Omega,\Omega') = \sum_{l=0}^{l=l_{\max}} \delta v_l(r)\delta(r-r')\hat{P}_l(\Omega,\Omega'), \tag{3}$$

where $\delta v_l(r) = v_l(r) - v_{l\mathrm{ref}}(r)$ and $\hat{P}_l$, given in terms of spherical harmonics Y_{lm}, is

$$\hat{P}_l(\Omega,\Omega') = \sum_{-m}^{+m} Y_{lm}^*(\Omega) Y_{lm}(\Omega'). \tag{4}$$

The nonlocality is hence limited to the angular coordinates, while the radial coordinate is local. For this reason, this is also called the *semilocal* form of the pseudopotential. However, applying v_{nloc} on wave functions is computationally very demanding since in reciprocal space v_{nloc} is a full matrix and for a given number N of plane waves used in the expansion of the wave functions, one has to compute N^2 matrix elements for each l, and then one has to perform a matrix-vector multiplication, which scales as N^2.

A clever way to bypass this bottleneck was introduced by KB.[8] In fact, KB transformed the nonlocal part into

$$v^{\mathrm{KB}} = \sum_{lm} \frac{\delta v_l |\phi_{lm}\rangle\langle\phi_{lm}|\delta v_l}{\langle\phi_{lm}|\delta v_l|\phi_{lm}\rangle}, \tag{5}$$

where $\phi_{lm} = Y_{lm}(\Omega)R_l(r)$ are the atomic pseudo-wave-functions used in the construction of the PP. In this way the PP becomes fully nonlocal in real space and completely separable. Using the PP in the KB form, the number of matrix elements to be computed grows only linearly with N, and the subsequent actions on the wave functions are reduced essentially to vector-vector scalar products.

However, as mentioned above, using the KB form one has to take care of ghost states. *Ghost-free* KB pseudopotentials can be constructed at least in a limited energy range by choosing suitable reference components, by adjusting the cutoff radius r_c, and by changing the ionization of the initial reference configuration.

We have identified and monitored the ghost states through two different techniques: direct spectral investigation and analysis of the logarithmic derivatives.[24,25] The latter are computed as

$$D_l(\epsilon,\bar{r}) = \frac{d}{dr}\ln u_l(\epsilon,r)|_{r=\bar{r}}, \tag{6}$$

where u_l is the radial atomic pseudo-wave-function. By construction, $D_l(\epsilon,\bar{r})$ for $\bar{r} \geq r_c$ is the same for the pseudo- and the all-electron atoms at the reference energy ϵ.[42] The logarithmic derivatives are used as a test of the transferability of the pseudopotential, i.e., its validity in different chemical environments.

B. Set of pseudopotentials considered

The set of silicon pseudopotentials considered in our study includes the following:

(a) One pseudopotential constructed with the standard partitioning between core and valence, i.e., by putting the $n=1$ and $n=2$ electron shells in the core. This pseudopotential will be called *standard* in the following.

(b) One pseudopotential generated with inclusion of the $2s$ and $2p$ electrons (outer-core states) in the valence (only the two $1s$ electrons remain in the core). In this case, this PP will be named *outer-core*.

In particular, independently of the core-valence partition chosen, we have used two different initial electronic configurations to construct the pseudopotential: (i) a neutral atom configuration ($1s^2 2s^2 2p^6 3s^2 3p^2 3d^0$) and (ii) an ionized-excited atom configuration ($1s^2 2s^2 2p^6 3s^1 3p^{0.75} 3d^{0.25}$) which corresponds to that proposed by Bachelet *et al.*[5]

In Table I a summary of the parameters chosen for the different atomic configurations is reported. We have used excited atomic configurations to generate the d component because the corresponding atomic wave functions are unbound in the atomic ground state. For the standard pseudo-

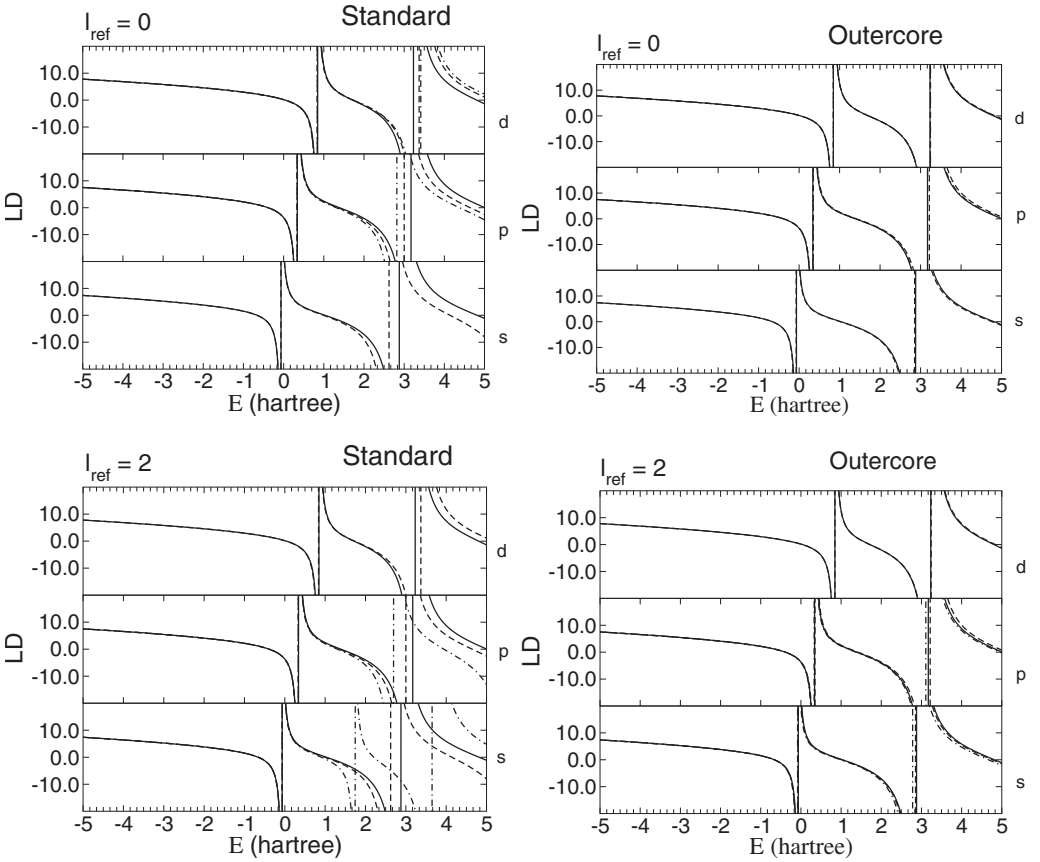

FIG. 1. Logarithmic derivatives of the s, p, and d components of our standard and outer-core pseudopotentials, in both their semilocal (dashed lines) and separable (KB) (dot-dashed lines) forms compared with their all-electron counterparts (solid lines). Results for different reference components ($l_{\mathrm{ref}}=0$ and $l_{\mathrm{ref}}=2$) are reported in the top and bottom parts of the figure, respectively. Note the large energy scale, ranging from −5.0 to 5.0 hartree.

potentials, both the fully nonlocal Kleinman-Bylander (separable) and the BHS (semilocal) forms have been considered and tested.

In all cases, as discussed above, a reference component $v_{l\mathrm{ref}}$ has been chosen for the local part of the pseudopotential, and all components v_l for $l \geq l_{\mathrm{max}}$ are set equal to $v_{l\mathrm{ref}}$. The choice of the most appropriate reference is not trivial, particularly in the Kleinman-Bylander case, where the appearance of ghost states is often triggered by the choice of $v_{l\mathrm{ref}}$. In the case of silicon most applications use $l_{\mathrm{max}}=l_{\mathrm{ref}}=2$, in which case only the $l=0$ and $l=1$ projectors have to be considered. However, there is no physical reason to assume the d angular component to be more representative of the high-l components than, e.g., the s component.[43] For this reason, we include in our analysis the results of calculations performed by choosing different l_{ref}, ranging from $l=0$ to $l=2$.

III. LOGARITHMIC DERIVATIVES, GROUND-STATE PROPERTIES, AND KOHN-SHAM BAND-STRUCTURE RESULTS

The logarithmic derivatives $D_l(\epsilon)$ have been analyzed for all the PPs considered in this paper, looking into an energy region extended as much as 100 eV above and below the Fermi energy. In the high-energy region ghost states are unavoidable, and they can enter in our calculations of the spectra.

In Fig. 1 we show the resulting $D_l(\epsilon)$ as a function of energy, comparing all-electron to PP results. As a matter of fact, choosing an s or p reference yields better results for the Kleinman-Bylander separation. The outer-core pseudopotential, on the other hand, gives LD very close to the all-electron ones in both the semilocal and the fully nonlocal cases, and for all possible choices of l_{ref}. However, the outer-core PP is harder; i.e., it requires a much larger set of plane waves to converge (125 hartree instead of the 15 hartree which is required for the standard PP).

It is important to note that in the case of the standard PP taking $l_{\mathrm{ref}}=2$ the LDs are quite bad beyond about 1.0 hartree above the zero energy reference. This behavior is acceptable for ground-state calculations because energies in that range are not involved, whereas they might create problems for excited-state calculations.

The following step is the analysis of the influence of the PP on the usual ground-state properties, such as the equilibrium lattice constant. Results, as displayed in Table II, show that the choice of $v_{l\mathrm{ref}}$ has a negligible effect, as expected. The outer-core PP produces better result than the standard PP. In fact, the lattice constant for an outer-core calculation is closer to the all-electron result in agreement with the work of Fiorentini *et al.*[44] In order to eliminate all the possible

TABLE II. Influence of the choice of the pseudopotential local reference component on the calculated equilibrium lattice constant of silicon. The separable form has been used in all six cases. The experimental value is 10.26 a.u.

Lattice parameter	$l_{ref}=0$ (a.u.)	$l_{ref}=1$ (a.u.)	$l_{ref}=2$ (a.u.)
Standard	10.178	10.180	10.170
Outer-core	10.250	10.250	10.249

sources of deviations in the spectra, which can be on the same order as the differences we are looking at, we perform all calculations of electronic properties at the experimental lattice constant, i.e., 10.26 a.u. for silicon and 8.24 a.u. for SiC. We have checked for silicon that using the theoretical lattice constants for our two pseudopotentials, instead of the experimental one, does not change the conclusions of this paper.

Up to this point all the considered PPs behave well for ground-state calculations. We are now interested in understanding their influence on spectroscopic quantities, which are usually constructed starting from Kohn-Sham eigenvalues and eigenfunctions. The latter have been computed for an unusually extended energy range, up to about 100 eV above the Fermi level, as needed for spectroscopic quantities. In fact, quantities such as the macroscopic dielectric function and the self-energy are constructed as infinite sums over states, involving virtual or real transitions.

To understand the differences, individual eigenvalues at the Γ point are analyzed in Figs. 2 and 3. The energy region is chosen around 60–90 eV above the Fermi level, a region where larger differences appear.

First evidence is that for the standard PP (Fig. 2, top) the influence of the choice of l_{ref} is much stronger than in the case of the outer-core PP (Fig. 2, bottom). The former can in fact be considered closer to an all-electron description. Hence it shows a better transferability (as demonstrated by the LD shown in Fig. 1), at the price of requiring a much larger number of plane waves to converge.

Furthermore, Fig. 3 compares the behaviors of the semilocal and the separable forms of the standard PP at fixed l_{ref}, showing also results from the outer-core PP. Assuming the latter as reference, results obtained using the separable form of the standard PP appear to be worse than those obtained using the semilocal form, with some dependence on l_{ref}. Indeed $l_{ref}=0$ gives a more stable behavior and better agreement between the separable and the semilocal forms. Choosing $l_{ref}=2$ can induce a visible scattering of some eigenvalues, as shown in Fig. 3 (top and central panels for the Γ point, and lower panel for a point of lower symmetry in the reciprocal space).

The simplest quantity involving a sum over states is the electronic density of states (DOS), for both occupied and empty states. No visible differences appear in the DOS of the occupied states nor in the lowest conduction states. Hence we only plot the range above 35 eV, where differences start to become visible. Differences between the semilocal and the separable forms of the same PP, at fixed reference component, are plotted for $l_{ref}=0$ in Fig. 4 and for $l_{ref}=2$ in Fig. 5.

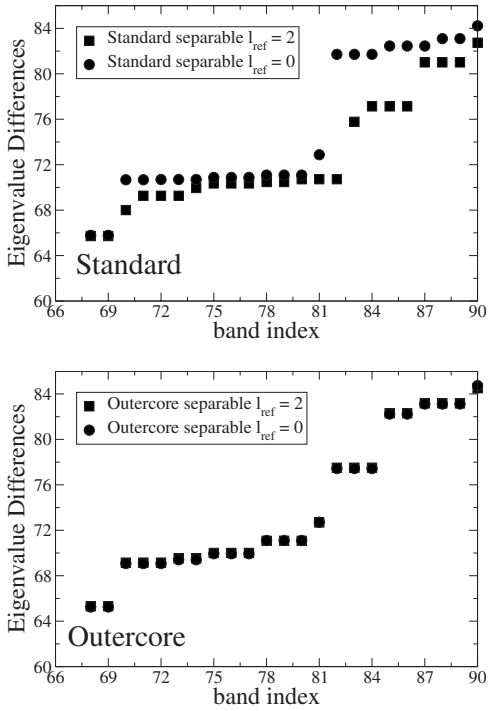

FIG. 2. Effects of the pseudopotential choice on individual KS-LDA eigenvalues of bulk Si at the Γ point in the high-energy region (60 eV above the Fermi level). Top panel: Influence of a change in the local reference component for the case of the standard pseudopotential used in its fully separable form. Bottom panel: Same as top panel, but for the outer-core pseudopotential. Results for $l_{ref}=0$ (points) and $l_{ref}=2$ (squares) are shown in both panels.

Consistent with the findings for single eigenvalues, the influence of l_{ref} is smaller for the PP in its semilocal form, while differences between the semilocal and the separable forms of the PP are amplified when the *d* reference component is chosen (note that $l_{ref}=2$ is another choice adopted because it reduces the computational cost). As a result, the choice of l_{ref} has a clear influence on the calculated DOS above 35 eV: the eigenvalues are affected, leading to visible change in the DOS.

Finally the quality of the corresponding eigenvectors has to be investigated. The influence of the PP on the KS eigenvectors has been analyzed through a direct comparison of two sets of eigenfunctions. To this end, we have computed the scalar products between two sets of low-energy eigenvectors, obtained with the semilocal and the separable forms. Only deviations of 1% from orthonormality were found.

IV. QUASIPARTICLE ENERGIES: *GW* CORRECTIONS TO THE KS-LDA BAND STRUCTURE

Realistic band structures are given by the poles of the one-particle Green's function, i.e., by *quasiparticle energies*, E^{QP}. The latter can be calculated through the electron self-energy Σ, a nonlocal and energy-dependent operator. The *GW* approximation[41] for computing Σ is nowadays the standard approach to including many-body effects in band-structure calculations.

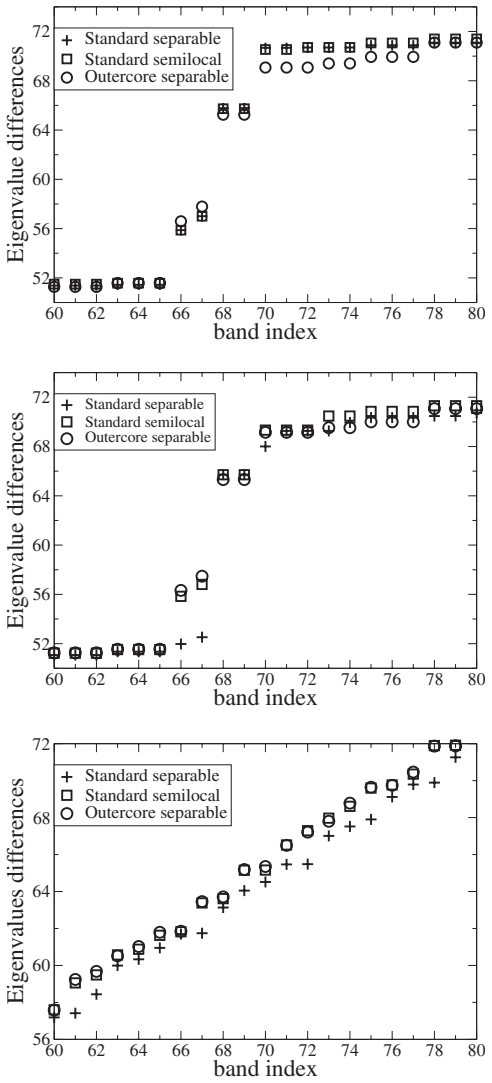

FIG. 3. Top panel: High-energy KS-LDA eigenvalues for bulk Si at the Γ point for the standard pseudopotential in semilocal (square) and separable forms (crosses), compared with results using the outer-core pseudopotential in its separable form (circle). $l_{\mathrm{ref}}=0$ has been used throughout. Central panel: Same as top panel, but using $l_{\mathrm{ref}}=2$ throughout. Bottom panel: Same as the central panel, but showing eigenvalues at a lower-symmetry **k** point [Baldereschi point (Ref. 45)].

In this approach, the self-energy operator, which is the proper "potential" acting on an excited electron or a hole in the system, is calculated as $\Sigma=iGW$, where G is the one-particle Green's function and W is the screened Coulomb interaction. Quasiparticle energies are usually obtained within first-order perturbation theory as $\epsilon_i^{GW}=\epsilon_i^{\mathrm{KS}}+[1/(1-\partial\Sigma/\partial\epsilon)]\langle\phi_i^{\mathrm{KS}}|\Sigma^{GW}(\epsilon_i^{\mathrm{KS}})-v_{\mathrm{xc}}|\phi_i^{\mathrm{KS}}\rangle$. In actual calculations, the one-particle Green's function and the screened Coulomb interaction are most often obtained starting from DFT-LDA pseudopotential-based calculations.

In this paper we have used this G_0W_0 approximation, where DFT-LDA single-particle orbitals (ϕ_i^{KS}) and energies (ϵ_i^{KS}) are hence used for building both

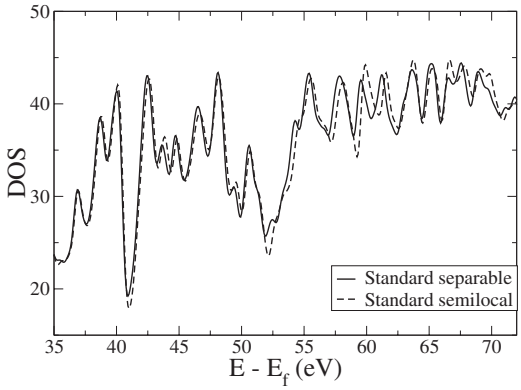

FIG. 4. Comparison between the LDA Kohn-Sham silicon DOSs calculated with a standard pseudopotential using its semilocal form (dashed line) and using its separable (KB) form (solid line). The reference component is taken as $l_{\mathrm{ref}}=0$ in both cases.

$$G_0(\mathbf{r},\mathbf{r}',\omega)=\sum_i \frac{\phi_i^{\mathrm{KS}}(\mathbf{r})\phi_i^{\mathrm{KS}*}(\mathbf{r}')}{\omega-\epsilon_i^{\mathrm{KS}}+i\eta\,\mathrm{sgn}\,(\epsilon_i^{\mathrm{KS}}-\mu)}, \tag{7}$$

with μ as the chemical potential, and the independent-particle linear polarizability

$$\chi_0^1(\mathbf{r},\mathbf{r}',\omega)=\sum_{ij}(f_i-f_j)\frac{\phi_i^{\mathrm{KS}*}(\mathbf{r})\phi_j^{\mathrm{KS}}(\mathbf{r})\phi_j^{\mathrm{KS}*}(\mathbf{r}')\phi_i^{\mathrm{KS}}(\mathbf{r}')}{\omega-(\epsilon_i^{\mathrm{KS}}-\epsilon_j^{\mathrm{KS}})+i\eta}, \tag{8}$$

where $i\eta$ is a small imaginary part.

The screened Coulomb interaction is obtained as $W=\varepsilon^{-1}v$, where v is the bare Coulomb potential and

$$\varepsilon=1-v\chi_0^1 \tag{9}$$

is the dielectric matrix in the random-phase approximation (RPA).

Containing wave functions and energies, both $G_0(\mathbf{r},\mathbf{r}',\omega)$ and $\chi_0^1(\mathbf{r},\mathbf{r}',\omega)$ are sensitive to the different pseudopotential choices. These states considered in Eqs. (7) and (8) include those far from the Fermi level for which the validity of the pseudopotential has been brought into question.

Furthermore *GW* energies are often used as input for other

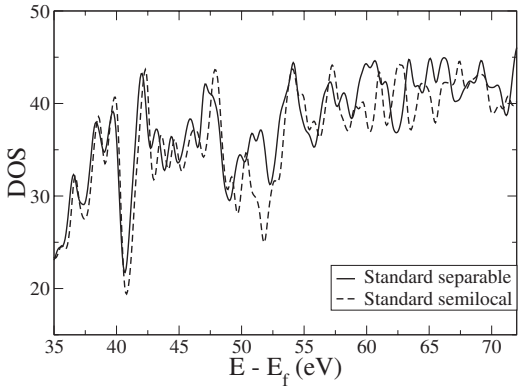

FIG. 5. Same as Fig. 4, but using $l_{\mathrm{ref}}=2$ in both the semilocal and separable forms of our standard pseudopotential.

TABLE III. Calculated Kohn-Sham LDA band gaps for silicon, with our standard and outer-core pseudopotentials, compared with pseudopotential and all-electron results from several other works. "Present work" results are those for $l_{\mathrm{ref}}=0$.

Si LDA	$\Gamma_c-\Gamma_v$	X_c-X_v	L_c-L_v	$X_c-\Gamma_v$	$L_c-\Gamma_v$
		PP method			
Present work, standard	2.56	3.47	2.63	0.64	1.44
Ref. 14	2.56	3.53	2.67	0.66	1.46
Ref. 46	2.57	3.43	2.64	0.65	1.47
Ref. 47	2.57			0.60	1.51
Ref. 48	2.59			0.65	1.47
Ref. 49	2.57			0.65	1.46
Ref. 50	2.57		2.75		
Ref. 51	2.58		2.63		
Ref. 9	2.55	3.48	2.69		
Present work, outer-core	2.52	3.42	2.53	0.56	1.33
Ref. 52	2.52			0.60	
		All-electron method			
Ref. 53	2.55	3.49	2.62	0.65	1.43
Ref. 54					
Ref. 55	2.53				
Ref. 31	2.53			0.65	1.52
Ref. 33	2.54	3.46	2.63	0.61	1.44

spectroscopic calculations, such as *ab initio* exciton calculations within the Bethe-Salpeter approach. A quantitative understanding of the limitations inherent to the DFT-LDA starting point is then even more crucial.

In the following we show the results obtained by performing standard G_0W_0 calculations based on the DFT-LDA electronic structure computed using the different pseudopotentials. Our results for the standard and the outer-core PPs relative to the Kohn-Sham LDA band gaps of bulk silicon are within the scattering of available PP and all-electron calculations from literature, as shown in Table III. There is an overall weak tendency of decrease in the gaps when the core states are included.

To converge *GW* results for the standard (outer-core) pseudopotential, we had to use 411 (12 039) plane waves for the wave functions and polarization matrices 283×283 (869×869) in the plane-wave basis. In both cases, we included 146 empty bands and 256 **k** points in the full Brillouin zone (BZ). All calculations have been done within the standard plasmon-pole approach.[56]

A first remarkable result is that changing the reference component or using a PP in its semilocal or separable form has a very little influence on the resulting QP corrections. Table IV shows our results for the quasiparticle-corrected Γ-point band gap of bulk silicon, together with the corresponding *GW* corrections. The differences are on the order of meV, i.e., only on the fourth significant digit. Since we consider that our results are precise within 50 meV, such differences are completely negligible. This robustness of *GW* corrections with respect to changes in the high-energy part of the KS spectrum suggests that the states far from the Fermi level could be quite safely approximated by using some kind of simplified model, without affecting the results.

The only significant differences induced by changing the pseudopotential scheme are found between the standard and the outer-core PPs since in the latter the calculated QP gaps are, on average, slightly smaller. All the values lie within the range of the different theoretical (PA and all-electron) and experimental results from literature as shown in Table V. As at the LDA level, the inclusion of the outer-core states decreases the gaps. This effect is stronger in the *GW* results than for the LDA gaps.

In the work of Tiago *et al.*[52] a pseudopotential with core states was used, generated from an initial electronic configuration different with respect to the one we have used for our outer-core PP. If we compare our results at the Γ point for the outer-core PP with their results, we obtain a value smaller by 0.15 eV. What Tiago *et al.*[52] obtained for Γ seems to be more similar to a standard PP calculation. However, their result for

TABLE IV. Influence of the choice of the local reference component on the quasiparticle band gap: $E_{\mathrm{gap}}^{\mathrm{QP}}$ of bulk silicon at the Γ point (first row). The second row shows the *GW* corrections, i.e., $E_{\mathrm{gap}}^{\mathrm{QP}}-E_{\mathrm{gap}}^{\mathrm{LDA}}$.

	Separable			Semilocal		
	$l_{\mathrm{ref}}=0$ (eV)	$l_{\mathrm{ref}}=1$ (eV)	$l_{\mathrm{ref}}=2$ (eV)	$l_{\mathrm{ref}}=0$ (eV)	$l_{\mathrm{ref}}=1$ (eV)	$l_{\mathrm{ref}}=2$ (eV)
$E_{\mathrm{gap}}^{\mathrm{QP}}$	3.233	3.232	3.231	3.232	3.232	3.229
$\Delta E_{\mathrm{gap}}^{GW}$	0.675	0.675	0.677	0.675	0.674	0.676

TABLE V. Calculated G_0W_0 band gaps for silicon with our standard and outer-core pseudopotentials, compared with pseudo- and all-electron results from several other works. "Present work" is shown for $l_{\mathrm{ref}}=0$. In parentheses we report the corresponding LDA gaps.

Si *GW*	$\Gamma_c-\Gamma_v$	X_c-X_v	L_c-L_v	$X_c-\Gamma_v$	$L_c-\Gamma_v$
			PP method		
Present work, standard	(2.56) 3.23	4.19	3.30	1.33	2.10
Ref. 14	(2.56) 3.25	4.27	3.38	1.31	2.13
Ref. 46	(2.57) 3.36	4.36	3.44	1.43	2.19
Ref. 47	(2.57) 3.27		3.44	1.44	2.27
Ref. 48	(2.59) 3.35			1.31	
Ref. 49	(2.57) 3.20			1.29	2.08
Ref. 50	(2.57) 3.30		3.49		2.30
Ref. 51	(2.58) 3.24	4.14	3.31	1.34	2.14
Ref. 9	(2.55) 3.23	4.18	3.38	1.35	2.18
Present work, outer-core	(2.52) 3.09	3.96	3.07	1.00	1.84
Ref. 52	(2.52) 3.24			1.18	
			All-electron method		
Ref. 53	(2.55) 3.30	4.17	3.41	1.14	2.15
Ref. 54	3.12				
Ref. 55	(2.53) 3.12				
Ref. 57	3.19	4.10	3.35		
Ref. 31	(2.53) 3.13/3.17	4.13/4.17	3.41/3.42	1.15/1.20	2.16/2.17
Ref. 33	(2.54) 3.09	3.91	3.21	1.01	2.05
Expt.	3.05–3.40			1.25	2.1(2.4 ± 0.15)

the $X-\Gamma$ gap is closer to an all-electron calculation.

The scattering in all these results can be explained by the different pseudizations of the wave functions and the core-valence partition chosen. These effects have been analyzed by studying their influence on the matrix elements of the LDA Kohn-Sham exchange-correlation potential and of the self-energy operator. In Table VI the contributions from V_{xc} and from Σ_{xc} are separately compared for the standard and the outer-core PPs. Furthermore, for the outer-core PP we have performed a valence-only calculation, neglecting all the contributions from the core states for the screening and for the self-energy. The results are shown only for the Γ point as the same conclusions are valid also for X and L.

The correlation terms never differ by more than 0.1 eV in all three cases. The exchange terms—for both the Kohn-Sham potential and the self-energy—can differ by more then 1 eV between the standard and the outer-core PPs. Neglecting the core states (valence-only outer-core) results in a difference with the standard on the order of 0.2 eV. We obtain the same trend shown by Gómez-Abal *et al.*[58] in a work where an all-electron and an all-electron valence-only G_0W_0 calculation were compared with PP results.

The effect of the core polarization is important on the single terms of the self-energy, and it is at the origin of the differences between the exchange contributions in the two outer-core calculations. Nevertheless, when the G_0W_0 gap is calculated (Table VII) the gaps are almost unchanged by the inclusion of the core states. This is due to a cancellation in the exchange part between the self-energy and the Kohn-Sham potential. The correlation contribution is practically the same in all three cases. Thus the exchange term seems to be the main cause of the differences between the outer-core and the standard PPs in the calculation of the G_0W_0 gaps. To get a deeper insight, we have directly plotted some of the matrix elements entering the calculation of the exchange self-energy, which reads

TABLE VI. Comparison of the exchange and correlation contribution to the matrix elements of the self-energy and of the DFT-LDA exchange and correlation potential, computed with our three types of PPs.

	V_x	V_c	Σ_x	Σ_c
		Standard		
Γ_{HOMO}	−9.76	−1.50	−12.45	0.49
Γ_{LUMO}	−8.63	−1.42	−5.82	−4.06
		V.O. outer-core		
Γ_{HOMO}	−9.93	−1.50	−12.28	0.52
Γ_{LUMO}	−8.75	−1.43	−5.75	−4.01
		Outer-core		
Γ_{HOMO}	−11.73	−1.56	−14.00	0.51
Γ_{LUMO}	−10.13	−1.47	−7.02	−4.03

TABLE VII. Calculated quasiparticle gaps at Γ, X, and L for the standard, the valence-only outer-core, and the outer-core calculations, as well as the corresponding contributions to the gaps from the $V_{\mathrm{xc}}-\Sigma_x$, $V_x-\Sigma_x$, and $V_c-\Sigma_c$.

	$E_{\mathrm{gap}}^{\mathrm{QP}}$	$\Delta E_{\mathrm{gap}}^{GW}$	$V_{\mathrm{xc}}-\Sigma_x$	$V_x-\Sigma_x$	$V_c-\Sigma_c$
			Standard		
$\Gamma_c-\Gamma_v$	3.23	0.68	−5.42	−5.50	4.63
X_c-X_v	4.18	0.71	−6.22	−6.33	5.39
L_c-L_v	3.30	0.67	−5.69	−5.75	4.87
			V.O. outer-core		
$\Gamma_c-\Gamma_v$	3.09	0.57	−5.28	−5.35	4.60
X_c-X_v	3.97	0.55	−5.99	−6.10	5.38
L_c-L_v	3.13	0.61	−5.50	−5.56	4.78
			Outer-core		
$\Gamma_c-\Gamma_v$	3.09	0.57	−5.29	−5.38	4.63
X_c-X_v	3.96	0.54	−5.91	−6.11	5.42
L_c-L_v	3.07	0.55	−5.47	−5.52	4.81

$$\langle \phi_{\mathbf{k}_j j}|\Sigma_x|\phi_{\mathbf{k}_j j}\rangle = -\frac{4\pi}{V}\sum_{\mathbf{k}_i i}\theta(\mu-\epsilon_{\mathbf{k}_i i})\sum_{\mathbf{G}}\tilde{\rho}^{*}_{\mathbf{k}_i ij}(\mathbf{q}+\mathbf{G}) \times\frac{1}{|\mathbf{q}+\mathbf{G}|^2}\tilde{\rho}_{\mathbf{k}_i ij}(\mathbf{q}+\mathbf{G}). \quad (10)$$

In the above formula, $\tilde{\rho}_{\mathbf{k}_i ij}(\mathbf{q}+\mathbf{G})$ is the Fourier transform of a product between $\phi_{\mathbf{k}_j j}(\mathbf{r})$ and $\phi_{\mathbf{k}_i i}(\mathbf{r})$ which are Kohn-Sham wave functions. The plotted quantity is $M(\mathbf{q}+\mathbf{G})=\tilde{\rho}^{*}_{\mathbf{k}_i ij}(\mathbf{q}+\mathbf{G})\tilde{\rho}_{\mathbf{k}_i ij}(\mathbf{q}+\mathbf{G})$, as a function of the $\mathbf{G}$ vectors for the standard and the outer-core PPs.

Figure 6 shows $M(\mathbf{q}+\mathbf{G})$ for the valence bands and the bottom conduction band at the X point. Degenerate states are summed over. In general, the matrix elements for the standard PP are larger by about 1%.

In conclusion, the pseudization of the wave functions seems to play the main role in the explanation of the differences between the gaps calculated with our two pseudopotentials, with or without inclusion of the core states, when using the outer-core PP, and does not change the final results. On the other hand the contribution of correlation is very stable. As a further investigation we have also performed a calculation by using the screening from the standard PP calculation, but the wave functions and energies calculated with the outer-core PP. We obtain for Σ_c at Γ lowest unoccupied molecular orbital (LUMO) [highest occupied molecular orbital (HOMO) 0.50 (−4.00) to be compared with 0.51 (−4.03). For X and L the variations are on the same order.

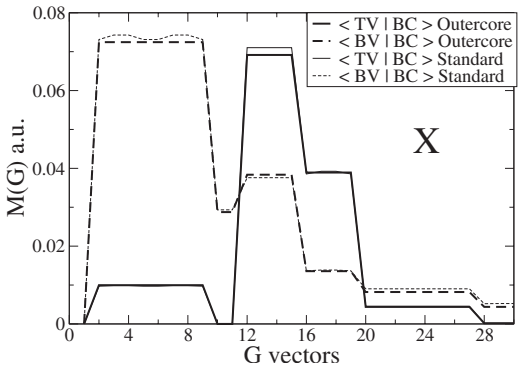

FIG. 6. Matrix elements entering Σ_x at the X point. The matrix elements have been calculated between the top valence (TV) [bottom valence (BV)] and the top conduction (TC) bands, and are shown as a function of the $\mathbf{G}$ vectors. The outer-core and the standard PPs are in their separable form.

All the GW results shown here were performed neglecting the effects of the $[V_{\mathrm{nl}},\mathbf{r}]$ commutator, discussed below, in the calculation of the screening because it is very time consuming. Their relative contribution, less than 1% on the band gap, can be reduced by improving the $\mathbf{q}$-point sampling of the Brillouin zone since it depends only on the $\mathbf{q}=0$ term. Moreover, all our GW calculations are performed at the G_0W_0 level, i.e., in a non-self-consistent scheme.

Most of the calculations in literature adopt this G_0W_0 scheme since full self-consistency, besides being numerically very heavy, has been shown in some cases to lead to a worsening of the results.[59,60] Self-consistency, using a static approach for the self-energy, tends to increase the GW gaps.[49,61]

On the other side, all-electron schemes do not suffer from the problems of the core-valence partitioning. The improvement in this direction is found for the outer-core PP which has been shown to reduce the gaps with respect to standard PA results. The reduction in the gaps leads to worse agreement with experimental results, even if the treatment of semiconductors is more consistent, as also shown by Sharma *et al.*[62] This means that there may be a certain cancellation between the effects of the PA and the non-self-consistency of the G_0W_0 calculation as proposed by Ku and Eguiluz.[55]

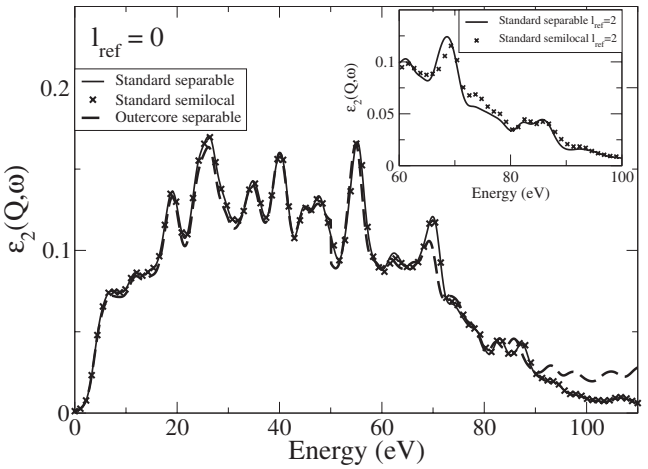

FIG. 7. Effects of the pseudopotential choice on the calculated imaginary part of the finite-**Q** macroscopic dielectric function of bulk silicon. Results obtained with the standard pseudopotential used in the semilocal and separable forms (stars and light solid line, respectively) and for the outer-core pseudopotential (solid line) with $l_{\mathrm{ref}}=0$ are reported. In the inset, $l_{\mathrm{ref}}=2$ is shown for the standard pseudopotential. The **Q** value is **Q**=1.86 a.u., and a grid of 32 (shifted) **k** points has been employed.

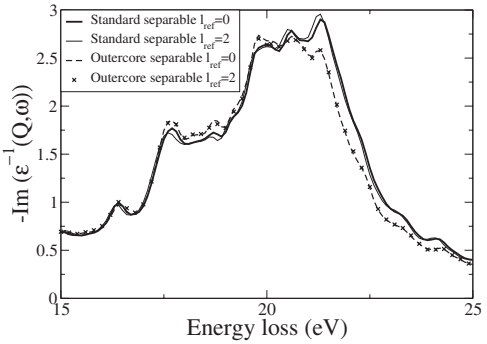

FIG. 8. Effects of the pseudopotential choice on the calculated finite-**Q** loss function of bulk silicon. Results obtained with the standard and the outer-core PPs used in their separable form are compared for different choices of l_{ref}. Standard (outer-core): $l_{\mathrm{ref}}=0$ solid line (dashed line) and $l_{\mathrm{ref}}=2$ light solid line (crosses). The transferred momentum **Q** is 0.53 a.u.

V. SPECTRA

In this section we consider PP effects on theoretical spectra. We study both the optical absorption spectra, which are given by the imaginary part of the dielectric function in the limit of vanishing momentum transfer, and the electron-energy-loss spectra for transferred momentum **Q**, given by $-\mathrm{Im}[\varepsilon^{-1}(\mathbf{q},\omega)]_{\mathbf{GG}}$, where **q** lies in the first Brillouin zone, **G** is a reciprocal-lattice vector, and $\mathbf{Q}=\mathbf{q}+\mathbf{G}$.

We present results within the RPA, where the dielectric matrix $\varepsilon(\mathbf{q},\omega)_{\mathbf{GG}}$ is given by Eq. (9). As we focus on the effects of the PA, the crystal local-field effects are not included (neglecting the off-diagonal elements of the microscopic dielectric matrix in reciprocal space). The error due to neglecting the local-field effects is known to be small in both Si and SiC.[63,64] The resulting simplified expression of the imaginary part of the macroscopic dielectric function $\varepsilon_2=v\chi_0$ allows us to analyze directly the contribution of individual valence-conduction transitions to the absorption spectra.

The imaginary part of the dielectric function for bulk silicon for **Q**=1.86 a.u. along the [110] direction is shown in Fig. 7 for the standard and the outer-core pseudopotentials.[65] In the case of the standard PP, results using both the semilocal and separable forms are shown together with the outer-core for $l_{\mathrm{ref}}=0$. Differences remain quite small, mainly appearing for the separable PP used with $l_{\mathrm{ref}}=2$ (inset starting from 60 eV), consistent with our findings on the eigenvalues.

In Fig. 8 we show an example of calculated loss spectra at **Q**=0.53 a.u. along the [111] direction, demonstrating the influence of a change in the reference component. Spectra in this range of **Q** are clearly quite independent of the choice of l_{ref}. Only for very large **Q** some differences appear because spectra become more sensitive to small changes in the high-energy electronic response. The main differences among these spectra are due to the inclusion of the outer-core states in the pseudopotential. The same effect is shown, for higher **Q**, in Fig. 9, where silicon $2p$ levels are present only for the outer-core (the respective transitions are obviously missing in the calculation with the standard PP).

In the case of the outer-core PP we have also investigated if the presence of the high-energy electronic transitions involving the outer-core (deep) electron levels induces a visible effect on the valence part of the loss spectra. A calculation (not shown) of loss spectra using the outer-core PP, either explicitly including or excluding the outer-core levels from the calculation of the macroscopic dielectric function, shows that this is not the case. The differences in the loss function at low energies due to the core polarization are rather small in the case of silicon. The only strong difference in the loss spectra is the $L_{2/3}$ absorption edge due to the presence of the outer-core states. Comparison with experimental spectra shows that the energy for the edge is underestimated by about 10 eV.

This can be explained in view of the DFT-LDA band structure. The binding energy of the Si $2p$ electrons is underestimated by about 10% (our results give −89.4 eV measured from the valence-band maximum by using $l_{\mathrm{ref}}=0$, and 89.7 eV by using $l_{\mathrm{ref}}=2$). The energy difference corresponds

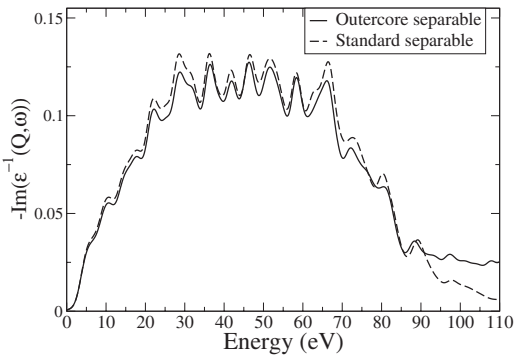

FIG. 9. Bulk silicon loss function for **Q**=1.86 a.u., calculated using the outer-core (solid line) and the standard (dashed line) pseudopotentials with $l_{\mathrm{ref}}=0$.

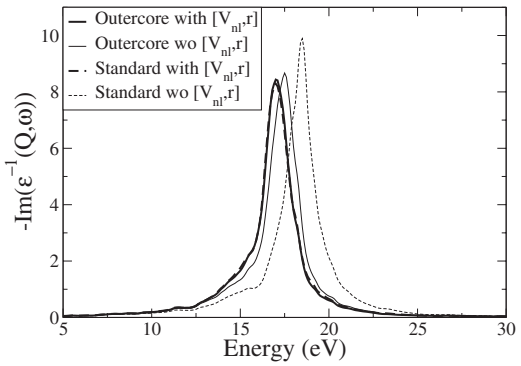

FIG. 10. Influence of the inclusion of the $[V_{\mathrm{nl}},\mathbf{r}]$ commutator on the computed loss function of bulk silicon at $\mathbf{Q}=0$, for both the standard pseudopotential (dashed line) and the outer-core pseudopotential (solid line). Dark (light) lines refer to calculations with (without) including the commutator. $l_{\mathrm{ref}}=0$ has been used throughout. The standard and the outer-core PPs are in their separable form.

roughly to the self-energy corrections found for these states by Rohlfing *et al.*[66]

For vanishing momentum transfer, the analysis of theoretical spectra deserves additional care due to the above-mentioned problem of the nonzero commutator between a nonlocal PP and the position operator $[V_{\mathrm{nl}},\mathbf{r}]$. In fact, a correct inclusion of the latter turns out to give rise to much larger effects on the calculated loss spectra than those due to the inclusion of outer-core electrons or to the change in the local reference component.

Figure 10 shows that neglecting the commutator can introduce changes in the plasmon energy by as much as 2 eV. However including the contribution from $[V_{\mathrm{nl}},\mathbf{r}]$ leads to very stable results with a plasmon peak much more independent of the pseudopotential choice. As a consequence of this, calculations which do not consider the commutator will be clearly affected by a degree of arbitrariness linked to the choice of the pseudopotential details (reference component and separable or semilocal form). The largest effect is found in the case of the standard pseudopotential used in its separable form. The outer-core pseudopotential, however, minimizes the effect of the commutator since it is closer to an all-electron description and the nonlocality has a lesser effect. The calculation of dipole matrix elements in the all-electron case would imply no nonlocal contribution at all.

The importance of the $[V_{\mathrm{nl}},\mathbf{r}]$ commutator in a correct evaluation of the position of the peaks of the inverse dielectric function can be understood as follows. An error in the evaluation of the matrix elements will affect, to first order,

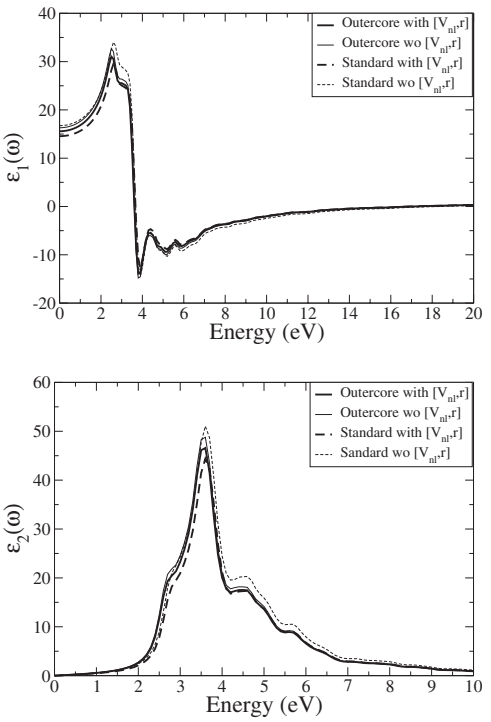

FIG. 11. Influence of the inclusion of the $[V_{\mathrm{nl}},\mathbf{r}]$ commutator on the dielectric function of bulk silicon at $\mathbf{Q}=0$, for both a standard pseudopotential (dotted line) and an outer-core pseudopotential (solid line). Dark (light) lines refer to calculations with (without) including the commutator. $l_{\mathrm{ref}}=0$ has been used throughout. The standard and the outer-core PPs are in their separable form.

only the intensity of the real and the imaginary parts of the dielectric function (Fig. 11) without changing the peak positions (provided it is calculated in the independent-particle approximation and without local-field effects). However, when the inverse has to be computed to obtain the loss function, a change in the overall intensity of the imaginary part will give rise to a change in the position of the zero crossing of the real part and consequently of the maximum of the imaginary part of the inverse function.

VI. NONLINEAR ELECTRONIC RESPONSE

The expressions arising in the description of the nonlinear response are much more complex than their linear counterparts. Thus the effects introduced by the PA have to be considered carefully. In the following, we consider the second-order response function in the RPA in the vanishing $\mathbf{q}$ limit:

$$\chi_0^{(2)}(2\mathbf{q},\mathbf{q},\mathbf{q},\omega,\omega)=\frac{4}{V}\sum_{n,n',n'',\mathbf{k}}\frac{\langle\phi_{n,\mathbf{k}}|e^{-2i\mathbf{qr}}|\phi_{n',\mathbf{k}+2\mathbf{q}}\rangle}{(E_{n,\mathbf{k}}-E_{n',\mathbf{k}+2\mathbf{q}}+2\omega+2i\eta)}\left[(f_{n,\mathbf{k}}-f_{n'',\mathbf{k}+\mathbf{q}})\frac{\langle\phi_{n',\mathbf{k}+2\mathbf{q}}|e^{i\mathbf{qr}'}|\phi_{n'',\mathbf{k}+\mathbf{q}}\rangle\langle\phi_{n'',\mathbf{k}+\mathbf{q}}|e^{i\mathbf{qr}''}|\phi_{n,\mathbf{k}}\rangle}{(E_{n,\mathbf{k}}-E_{n'',\mathbf{k}+\mathbf{q}}+\omega+i\eta)}\right.$$
$$\left.+(f_{n',\mathbf{k}+2\mathbf{q}}-f_{n'',\mathbf{k}+\mathbf{q}})\frac{\langle\phi_{n',\mathbf{k}+2\mathbf{q}}|e^{i\mathbf{qr}'}|\phi_{n'',\mathbf{k}+\mathbf{q}}\rangle\langle\phi_{n'',\mathbf{k}+\mathbf{q}}|e^{i\mathbf{qr}''}|\phi_{n,\mathbf{k}}\rangle}{(E_{n'',\mathbf{k}+\mathbf{q}}-E_{n',\mathbf{k}+2\mathbf{q}}+\omega+i\eta)}\right]. \quad (11)$$

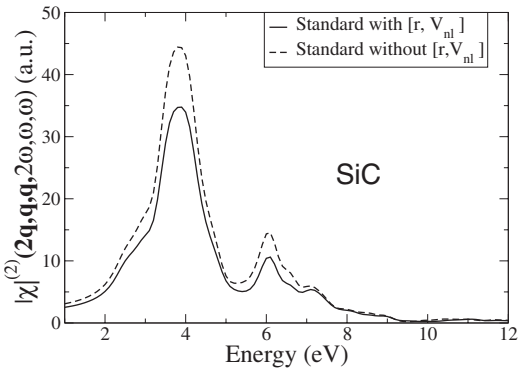

FIG. 12. Effects of the inclusion of the $[V_{\mathrm{nl}},\mathbf{r}]$ commutator on the calculated second-order susceptibility of bulk SiC, using a standard pseudopotential in its separable form and choosing $l_{\mathrm{ref}}=0$.

To the best of our knowledge, the effects of the PA on the calculations beyond the linear response have never been studied explicitly before, and the fact of having a triple summation over states (both occupied and empty), involving the product of three matrix elements, could cause this quantity to be more sensitive to the approximations used in its construction. The complexity of the χ_0^2 clearly gives rise to more subtle convergence issues compared to the linear case [see, e.g., Eq. (8)]. The required ingredients are, once again, independent-particle eigenvalues and eigenfunctions, which are taken from a pseudopotential-based electronic-structure calculation within DFT-LDA in the Kohn-Sham scheme.

Since bulk silicon, being centrosymmetric, has no second-order response, we performed our calculations for silicon carbide (SiC), which is one of the simplest nonlinear semiconductors thanks to its ionicity and its lack of inversion symmetry. Moreover, experimental and theoretical results on the SHG spectra are available for this material.

As in the case of the linear response discussed above, we have performed Kohn-Sham band-structure calculations within a standard plane-wave pseudopotential approach, using the ABINIT code,[67] and the nonlinear response calculations using the DP code.[68] The main convergence difficulty is found to be the **k**-point sampling. It was solved by using an off-symmetry-shifted grid of 256 **k** points in the full Brillouin zone. To converge the calculations 25 empty bands was required (i.e., up to about 10 eV above the Fermi energy), and 169 plane waves, corresponding to an energy cutoff of 5 hartree.

The effects induced by the pseudopotential choice turn out to be very small. Even a delicate quantity such as the second-order response turns out to be a little sensitive to the change in the local reference component of the pseudopotential. This result could be expected since only bands near to the Fermi energy are involved.

By contrast, the effects due to the inclusion of the $[V_{\mathrm{nl}},\mathbf{r}]$ commutator in the calculation of the dipole matrix elements are much larger, as shown in Fig. 12. As in the case of the linear response, the inclusion of the commutator gives rise (in the case of SiC) to a reduction in the spectral strength, but in this case the effect seems to be stronger.

VII. CONCLUSIONS

We have presented a detailed analysis of pseudopotential-induced effects in *ab initio* calculations in Si and SiC, including Kohn-Sham band structures, quasiparticle corrections, and electron-energy-loss and optical spectra in both the linear and the nonlinear regimes. Our results show that the usual (Kleinman-Bylander) pseudopotential scheme, originally developed for ground-state calculations, can be quite safely applied to excited-state calculations even when they involve summation over Kohn-Sham eigenvectors and eigenvalues up to 100 eV. The performance of the standard (valence-only) KB pseudopotential can be optimized by an appropriate choice of the local reference component. Inclusion of the outer-core states in the valence, however, leads to harder but more stable (i.e., less influenced by the reference component) pseudopotentials.

Kohn-Sham band structures computed using a PP in both its semilocal and fully nonlocal (KB) forms have shown that in the Kleinman-Bylander case the influence of the choice of the reference component is larger. Concerning *GW* quasiparticle corrections, our results indicate that fine details of the density of states and of the matrix elements do not play a critical role in the calculation. In particular, the variations in quasiparticle corrections computed within different PAs are always on the order of 0.1 eV. The pseudopotential including outer-core states, however, systematically yields results closer to those of all-electron calculations because of an improvement of the wave functions, even if the transitions involving the outer-core states are not important in these calculations. The relative stability of the *GW* results also suggests that simplified methods for treating the high-energy part of the Kohn-Sham spectrum could be applied.[69]

The relevant quantities such as the spectra have been found to be a little sensitive to the details of the PP construction. This also holds for the nonlinear response. However, our results for energy-loss spectra at vanishing momentum transfer show that the role of the $[V_{\mathrm{nl}},\mathbf{r}]$ commutator in the calculation of the matrix elements is important, and definitely more important than the role played by the choice of the pseudopotentials. The effect of $[V_{\mathrm{nl}},\mathbf{r}]$ is even stronger in the case of the nonlinear second-order response.

ACKNOWLEDGMENTS

This work was supported by the European Union through the NANOQUANTA Network of Excellence and the ETSF Integrated Infrastructure Initiative, as well as by ANR Project No. ANR-05-BLANC-0191-01-LSI 1718 and MIUR-PRIN2005 Ref. No. 2005028257. E.L. and H.-Ch.W. acknowledge financial support from the European Community through the Marie Curie Training Site, under Grant No. HPMT-CT-2001-00368. H.-Ch.W. acknowledges support from the European Union through the individual Marie Curie Intra-European Grant No. MEIF-CT-2005-025067.

[1] B. Arnaud, S. Lebègue, P. Rabiller, and M. Alouani, Phys. Rev. Lett. **96**, 026402 (2006).
[2] F. Bruneval, F. Sottile, V. Olevano, R. Del Sole, and L. Reining, Phys. Rev. Lett. **94**, 186402 (2005).
[3] E. Luppi, F. Iori, R. Magri, O. Pulci, S. Ossicini, E. Degoli, and V. Olevano, Phys. Rev. B **75**, 033303 (2007).
[4] W. Wełnic, S. Botti, L. Reining, and M. Wuttig, Phys. Rev. Lett. **98**, 236403 (2007).
[5] G. B. Bachelet, D. R. Hamann, and M. Schlüter, Phys. Rev. B **26**, 4199 (1982).
[6] D. R. Hamann, M. Schlüter, and C. Chiang, Phys. Rev. Lett. **43**, 1494 (1979).
[7] N. Troullier and J. L. Martins, Phys. Rev. B **43**, 1993 (1991).
[8] L. Kleinman and D. M. Bylander, Phys. Rev. Lett. **48**, 1425 (1982).
[9] A. Fleszar and W. Hanke, Phys. Rev. B **56**, 10228 (1997).
[10] R. W. Godby, M. Schlüter, and L. J. Sham, Phys. Rev. B **35**, 4170 (1987).
[11] R. W. Godby, M. Schlüter, and L. J. Sham, Phys. Rev. B **37**, 10159 (1988).
[12] M. S. Hybertsen and S. G. Louie, Phys. Rev. Lett. **55**, 1418 (1985).
[13] G. Onida, L. Reining, and A. Rubio, Rev. Mod. Phys. **74**, 601 (2002).
[14] W. G. Aulbur, L. Jönsson, and J. W. Wilkins, Solid State Phys. **54**, 1 (1999).
[15] S. Botti, F. Sottile, N. Vast, V. Olevano, L. Reining, H.-C. Weissker, A. Rubio, G. Onida, R. Del Sole, and R. W. Godby, Phys. Rev. B **69**, 155112 (2004).
[16] M. E. Casida, in *Recent Advances in Density Functional Methods, Part I*, edited by D. P. Chong (World Scientific, Singapore, 1995), p. 155.
[17] J. F. Dobson, in *Electronic Density Functional Theory: Recent Progress and New Directions*, edited by J. F. Dobson, G. Vignale, and M. P. Das (Plenum, New York, 1997).
[18] L. Reining, V. Olevano, A. Rubio, and G. Onida, Phys. Rev. Lett. **88**, 066404 (2002).
[19] I. G. Gurtubay, J. M. Pitarke, W. Ku, A. G. Eguiluz, B. C. Larson, J. Tischler, P. Zschack, and K. D. Finkelstein, Phys. Rev. B **72**, 125117 (2005).
[20] F. Sottile, M. Marsili, V. Olevano, and L. Reining, Phys. Rev. B **76**, 161103(R) (2007).
[21] H.-C. Weissker, J. Serrano, S. Huotari, F. Bruneval, F. Sottile, G. Monaco, M. Krisch, V. Olevano, and L. Reining, Phys. Rev. Lett. **97**, 237602 (2006).
[22] R. Leitsmann, W. G. Schmidt, P. H. Hahn, and F. Bechstedt, Phys. Rev. B **71**, 195209 (2005).
[23] The Wronskian theorem is obeyed by construction using semilocal pseudopotentials.
[24] X. Gonze, P. Kackell, and M. Scheffler, Phys. Rev. B **41**, 12264 (1990).
[25] X. Gonze, R. Stumpf, and M. Scheffler, Phys. Rev. B **44**, 8503 (1991).
[26] S. Baroni and R. Resta, Phys. Rev. B **33**, 7017 (1986).
[27] A. J. Read and R. J. Needs, Phys. Rev. B **44**, 13071 (1991).
[28] B. Adolph, J. Furthmüller, and F. Bechstedt, Phys. Rev. B **63**, 125108 (2001).
[29] P. E. Blöchl, Phys. Rev. B **50**, 17953 (1994).
[30] B. Arnaud and M. Alouani, Phys. Rev. B **63**, 085208 (2001).
[31] B. Arnaud and M. Alouani, Phys. Rev. B **62**, 4464 (2000).
[32] P. Puschnig and C. Ambrosch-Draxl, Phys. Rev. B **66**, 165105 (2002).
[33] S. Lebègue, B. Arnaud, M. Alouani, and P. E. Bloechl, Phys. Rev. B **67**, 155208 (2003).
[34] G. Kresse and D. Joubert, Phys. Rev. B **59**, 1758 (1999).
[35] H. Ch. Weissker, J. Furthmüller, and F. Bechstedt, Phys. Rev. B **64**, 035105 (2001).
[36] P. E. Blöchl, Phys. Rev. B **41**, R5414 (1990).
[37] H. Kageshima and K. Shiraishi, Phys. Rev. B **56**, 14985 (1997).
[38] A. F. Starace, Phys. Rev. A **3**, 1242 (1971).
[39] R. Del Sole and R. Girlanda, Phys. Rev. B **48**, 11789 (1993).
[40] J. L. P. Hughes and J. E. Sipe, Phys. Rev. B **53**, 10751 (1996).
[41] L. Hedin, Phys. Rev. **139**, A796 (1965).
[42] In the pseudopotential generation scheme, the reference energy is the energy at which the pseudo-wave-function and the all-electron wave function coincide.
[43] M. Meyer, G. Onida, M. Palummo, and L. Reining, Phys. Rev. B **64**, 045119 (2001).
[44] V. Fiorentini, M. Methfessel, and M. Scheffler, Phys. Rev. B **47**, 13353 (1993).
[45] A. Baldereschi, Phys. Rev. B **7**, 5212 (1973).
[46] M. Rohlfing, P. Krüger, and J. Pollmann, Phys. Rev. B **48**, 17791 (1993).
[47] M. S. Hybertsen and S. G. Louie, Phys. Rev. B **35**, 5585 (1987).
[48] E. L. Shirley, X. Zhu, and S. G. Louie, Phys. Rev. B **56**, 6648 (1997).
[49] F. Bruneval, N. Vast, and L. Reining, Phys. Rev. B **74**, 045102 (2006).
[50] R. W. Godby, M. Schlüter, and L. J. Sham, Phys. Rev. Lett. **56**, 2415 (1986).
[51] M. M. Rieger, L. Steinbeck, I. D. White, H. N. Rojas, and R. W. Godby, Comput. Phys. Commun. **117**, 211 (1999).
[52] M. L. Tiago, S. Ismail-Beigi, and S. G. Louie, Phys. Rev. B **69**, 125212 (2004).
[53] N. Hamada, M. Hwang, and A. J. Freeman, Phys. Rev. B **41**, 3620 (1990).
[54] T. Kotani and M. van Schilfgaarde, Solid State Commun. **121**, 461 (2002).
[55] W. Ku and A. G. Eguiluz, Phys. Rev. Lett. **89**, 126401 (2002).
[56] R. W. Godby and R. J. Needs, Phys. Rev. Lett. **62**, 1169 (1989).
[57] C. Friedrich, A. Schindlmayr, S. Blügel, and T. Kotani, Phys. Rev. B **74**, 045104 (2006).
[58] R. Gómez-Abal, X. Li, M. Scheffler, and C. Ambrosch-Draxl, Phys. Rev. Lett. **101**, 106404 (2008).
[59] W.-D. Schöne and A. G. Eguiluz, Phys. Rev. Lett. **81**, 1662 (1998).
[60] U. von Barth and B. Holm, Phys. Rev. B **54**, 8411 (1996).
[61] S. V. Faleev, M. van Schilfgaarde, and T. Kotani, Phys. Rev. Lett. **93**, 126406 (2004).
[62] S. Sharma, J. K. Dewhurst, and C. Ambrosch-Draxl, Phys. Rev. Lett. **95**, 136402 (2005).
[63] V. I. Gavrilenko and F. Bechstedt, Phys. Rev. B **54**, 13416 (1996).
[64] V. I. Gavrilenko and F. Bechstedt, Phys. Rev. B **55**, 4343 (1997).

[65] 32 k points for test purposes.
[66] M. Rohlfing, P. Krüger, and J. Pollmann, Phys. Rev. B **56**, R7065 (1997).
[67] The ABINIT code is a common project of the Université Catholique de Louvain, Corning Incorporated, and other contributors; see http://www.abinit.org
[68] The DP code is developed by the French node of the ETSF; see http://www.dp-code.org
[69] F. Bruneval and X. Gonze, Phys. Rev. B **78**, 085125 (2008).